Multiphase Flow and Poro-(Visco)-Elasto-Plastic Rheology: 3D GPU Implementation

Yury Alkhimenkov[1,2]*, Yury Podladchikov[2], Ruben Juanes[1]
[1] Massachusetts Institute of Technology, Cambridge, MA, USA; *yalkhime@mit.edu; yalkhime@gmail.com
[2] University of Lausanne, Switzerland

Introduction

Modeling the coupled processes of poromechanics (poro-elasto-plastic rheology) and two-phase fluids is crucial for understanding complex subsurface phenomena, including phase redistribution, deformation-induced flow dynamics, and mechanical instabilities. This study presents a high-performance computational framework that integrates quasi-static Biot equations with compressible two-phase transport and frictional plasticity. The model captures large-strain poro-elastoplastic behavior, and capillary pressure effects. To efficiently solve this coupled system, we employ a conservative finite-volume discretization combined with an accelerated pseudo-transient (APT) iterative solver, optimized for GPU architectures, achieving significant computational gains in large-scale simulations. Our results reveal the intricate interplay between mechanical deformation and fluid flow, capturing pressure evolution, strain localization, and saturation front propagation under varying conditions.

Symmetric conditions

In accordance with the general principles of thermodynamics, the coefficient matrix that governs the relationships between the divergences of solid velocity and Darcy fluxes with the time derivatives of pressures must be symmetric. Enforcing this symmetry leads to the following conditions:

$$\frac{D\phi_{f1}}{Dt} = -S_1 \frac{D\phi_s}{Dt}, \tag{1}$$

and

$$\frac{D\phi_{f2}}{Dt} = -S_2 \frac{D\phi_s}{Dt}. \tag{2}$$

These equations ensure the symmetry of the resulting 3×3 matrix, which is presented below. The symmetry condition is essential for the consistency of the coupled system, preserving the thermodynamically admissible structure of the governing equations. The total fluid pressure derivative is:

$$\frac{Dp_{ft}}{Dt} = S_1 \frac{Dp_{f1}}{Dt} + (1 - S_1)\frac{Dp_{f2}}{Dt}. \tag{3}$$

Note that such formulation of the total fluid pressure provides us with a simple matrix of coefficients that relate pressures and divergences

Model Setup

We employ the quasi-static Biot's poroelastic equations [1] to describe coupled porous-media two-phase flow and deformation. The governing equations include:

$$\left(\begin{pmatrix} \nabla_k v_k^s \\ \nabla_k q_k^{D1} \\ \nabla_k q_k^{D2} \end{pmatrix}\right) = -\beta_d \left(\begin{pmatrix} 1 & -\alpha S_1 & -\alpha S_2 \\ -\alpha S_1 & \beta_{22} & \beta_{23} \\ -\alpha S_2 & \beta_{32} & \beta_{33} \end{pmatrix}\right) \left(\begin{pmatrix} \frac{D^s \bar{p}}{dt} \\ \frac{D^{f1} p_{f1}}{dt} \\ \frac{D^{f2} p_{f2}}{dt} \end{pmatrix}\right). \tag{4}$$

By substituting the expressions for the time derivatives of densities and porosity into equations for divergences $\nabla_j v_j^s$, $\nabla_j q_j^{Dt}$, we obtain the following system of equations for compressibilities:

$$\left(\begin{pmatrix} \nabla_k v_k^s \\ \nabla_k q_k^{Dt} \end{pmatrix}\right) = -\beta_d \left(\begin{pmatrix} 1 & -\alpha \\ -\alpha & \frac{\alpha}{B^*} \end{pmatrix}\right) \left(\begin{pmatrix} \frac{D^s \bar{p}}{Dt} \\ \frac{D^f p_{ft}}{Dt} \end{pmatrix}\right) + \left(\begin{pmatrix} 0 \\ \beta_{23} \frac{Dp_c}{Dt} \end{pmatrix}\right), \tag{5}$$

where

$$\alpha = \frac{\beta_d - \beta_s}{\beta_d}, \quad B^* = \frac{\beta_s - \beta_d}{(\beta_s - \beta_{f1})\phi_{f1} + (\beta_s - \beta_{f2})\phi_{f2} - \beta_d + \beta_s}. \tag{6}$$

Fluid flow within the porous medium follows Darcy's law for two-phase flow:

$$q_i^{D1} = -\frac{k k_{r1}}{\eta_{f1}} \left(\nabla_i p_{f1} + g_i \rho_{f1}\right), q, \quad q_i^{D2} = -\frac{k k_{r2}}{\eta_{f2}} \left(\nabla_i p_{f2} + g_i \rho_{f2}\right). \tag{7}$$

The system is solved using an Accelerated Pseudo-Transient (APT) Method, a matrix-free iterative solver that ensures convergence to quasi-static solutions [2].

Numerical Simulations

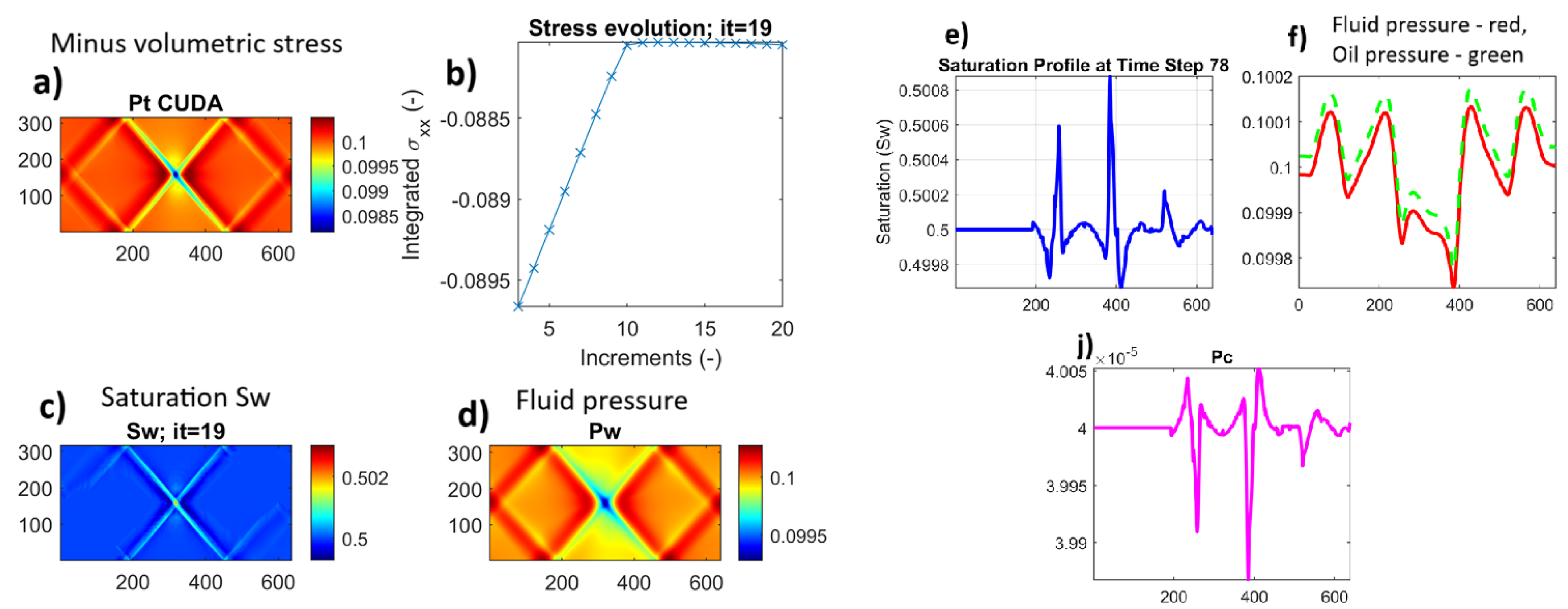

Figure 1: Two-dimensional simulation results illustrating strain localization and fluid redistribution. (a) Minus volumetric stress (total pressure). (b) Integrated stress evolution. (c) Fluid saturation S_w. (d) Fluid pressure P_w. (e) 1D saturation profile at one-third of the domain height. (f) 1D fluid pressure (red) and oil pressure (green). (j) Capillary pressure profile. Results show a clear shear band where total pressure, fluid pressure, and capillary pressure drop, while fluid saturation and porosity increase. Advection-driven flow dominates transport due to fluid pressure gradients.

3D Numerical Simulations

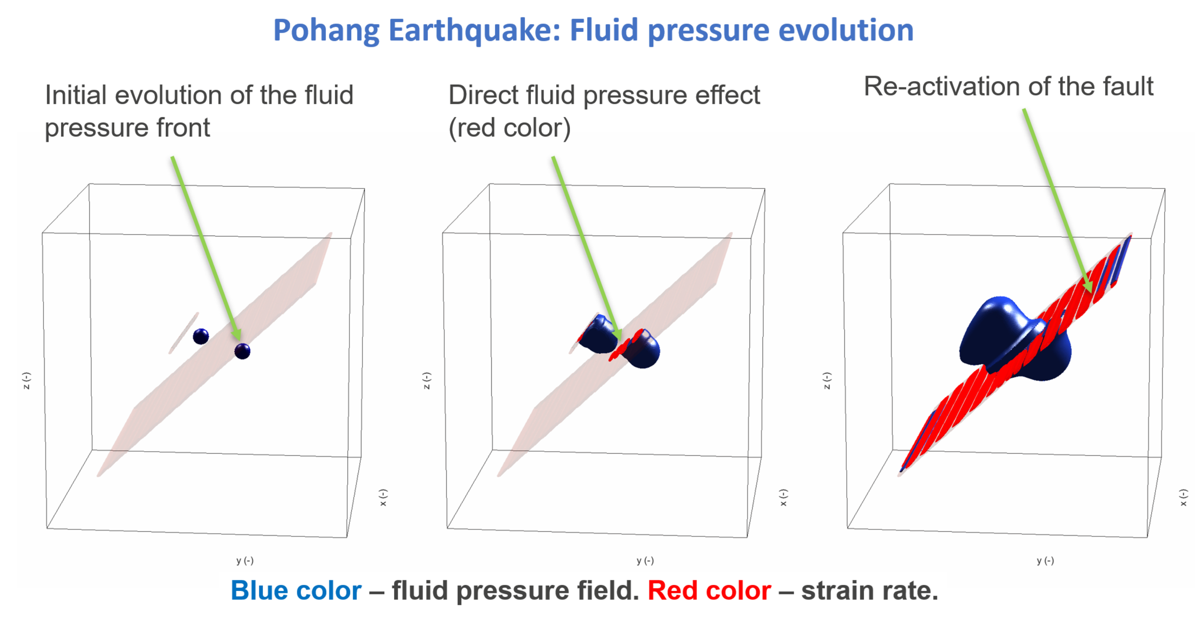

Figure 2: Fluid pressure evolution in settings close to the Pohang earthquake [3].

Performance

The solver demonstrates exceptional GPU performance: Achieves **120**× acceleration over CPU-based methods [4]

Conclusion

We present a high-performance numerical framework for fully coupled two-phase flow and poro-elasto-plasticity, leveraging GPU acceleration to enable large-scale simulations with high spatial and temporal resolution. The model integrates large-strain mechanics and capillary pressure effects, allowing for the accurate representation of fluid redistribution, strain localization, and poromechanical deformation.

References

[1] Maurice A Biot. Mechanics of deformation and acoustic propagation in porous media. *Journal of applied physics*, 33(4):1482–1498, 1962.

[2] Yury Alkhimenkov and Yury Y Podladchikov. Accelerated pseudo-transient method for elastic, viscoelastic, and coupled hydro-mechanical problems with applications. *Geoscientific Model Development Discussions*, 2024:1–35, 2024.

[3] Yury Alkhimenkov and Ruben Juanes. Numerical modeling of induced seismicity using graphical processing units (gpus). In *AGU Fall Meeting Abstracts*, volume 2023, pages S21F–0356, 2023.

[4] Yury Alkhimenkov. High-resolution gpu-based simulations of quasi-static poroelasticity: seismic attenuation and modulus dispersion in three-dimensional stochastic fracture networks. *Geophysical Journal International*, 240(2):1234–1253, 2025.